Electronic structure and magnetic properties of Li_2ZrCuO_4: A spin-$\frac{1}{2}$ Heisenberg system close to a quantum critical point

M. Schmitt,[1] J. Málek,[2,3] S.-L. Drechsler,[3] and H. Rosner[1]
[1]*Max-Planck-Institut für Chemische Physik fester Stoffe, Nöthnitzer Str. 40, D-01187 Dresden, Germany*
[2]*Institute of Physics, ASCR, Na Slovance 2, CZ-1822, Prague, Czech Republic*
[3]*Leibniz-Institut für Festkörper- und Werkstoffforschung Dresden, P.O. Box 270116, D-01171 Dresden, Germany*
(Received 25 June 2009; revised manuscript received 29 September 2009; published 11 November 2009)

Based on density-functional calculations, we present a detailed theoretical study of the electronic structure and the magnetic properties of the quasi-one-dimensional chain cuprate Li_2ZrCuO_4 (Li_2CuZrO_4). For the relevant ratio of the next-nearest-neighbor exchange J_2 to the nearest-neighbor exchange J_1 we find $\alpha=-J_2/J_1=0.22\pm0.02$ which is very close to the critical point at 1/4. Owing this vicinity to a ferromagnetic-helical critical point, we study in detail the influence of structural peculiarities such as the reported Li disorder and the nonplanar chain geometry on the magnetic interactions combining the results of local-density-approximation-based tight-binding models with LDA+*U*-derived exchange parameters. Our investigation is complemented by an exact diagonalization study of a multiband Hubbard model for finite clusters predicting a strong temperature dependence of the optical conductivity for Li_2ZrCuO_4.

DOI: 10.1103/PhysRevB.80.205111 PACS number(s): 71.20.−b, 75.30.Et

I. INTRODUCTION

Low-dimensional magnetism has always attracted great interest in solid-state physics and chemistry. Especially, the phase diagram of low-dimensional spin-$\frac{1}{2}$ lattices has been investigated extensively, both theoretically and experimentally. For low dimensions and spin-$\frac{1}{2}$, the influence of quantum fluctuations becomes crucial for the ground state of the system. The role of quantum fluctuations is even more pronounced if the system under consideration exhibits strongly frustrated interactions.

Taking only nearest-neighbor interactions into account, pure geometrical frustration in two dimensions (2D) can be realized by special symmetries, i.e., triangular or Kagomé lattices. Prominent real material realizations for such lattices are κ-$(BEDT\text{-}TTF)_2X$ (Ref. 1) and $ZnCu_3(OH)_6Cl_2$.[2] Another possibility to realize frustrated couplings are competing nearest-neighbor (NN) and next-nearest-neighbor (NNN) interactions. This way, the unfrustrated NN Heisenberg square lattice becomes frustrated by adding antiferromagnetic (AFM) interactions to NNN. The ground state of this model is determined by the ratio $\alpha=-J_2/J_1$ between NNN and NN exchange interaction. Including a tiny, but nonvanishing coupling between the magnetic planes that is always present in real materials, for small α an antiferromagnetic ground state is observed like in all undoped HTSC parent compounds.[3] For large α the so-called columnar order is expected, as found in Li_2VSiO_4 or Li_2VGeO_4.[4–8] Between these commensurably ordered phases, theory predicts a spin-liquid ground state. The possible realization of this spin-liquid ground state in $PbVO_3$ is presently under debate.[9,10]

In one dimension (1D), pure geometrical frustration due to NN exchange is impossible, but frustration by competing NN and NNN exchanges may occur in close analogy to the 2D square J_1-J_2 model. The phase diagram of this seemingly simple model is very rich. Depending on the frustration ratio α, a variety of ground states was observed in corresponding quasi-1D systems: (i) ferromagnetically ordered chains in Li_2CuO_2 (Ref. 11) ($0\leq\alpha\leq0.25$, within an effective single-chain analysis ignoring the antiferromagnetic interchain interaction[12]), (ii) helical order with different pitch angles in $LiVCuO_4$, $LiCu_2O_2$, and $NaCu_2O_2$ (Refs. 13–18) ($\alpha>0.25$) or (iii) spin gap behavior like in the famous spin-Peierls compound $CuGeO_3$ (Ref. 19) ($-\alpha>0.241$), where both exchange couplings are antiferromagnetic.

Very recently, large interest focused on chain systems that are close to the quantum critical point (QCP) at $\alpha=0.25$. In the vicinity of a QCP, the system is expected to answer in a pronounced way to small external perturbations such as magnetic fields or pressure. In addition, even very small additional exchange paths, especially the interchain coupling, become important for the magnetic properties of the system. A most promising compound to study the close vicinity to the QCP is Li_2ZrCuO_4, where a frustration ratio of $\alpha=0.29$ was reported from the evaluation of susceptibility and specific-heat data.[20] The expected strong field dependence of the specific heat from magnetic fields up to 9 T was observed, although the NN exchange J_1 was estimated to be rather large on the order of 300 K. The vicinity of Li_2ZrCuO_4 to the QCP was supported by preliminary band-structure calculations that obtained a frustration ratio $\alpha\sim0.23$.

In this paper, we report a detailed electronic structure study based on density-functional calculations. In particular, we investigate the influence of the experimentally observed Li disorder[21] for one of the crystallographic Li sites on the magnetic properties. We discuss the dependency of the exchange integrals and the frustration ratio α on the strong Coulomb repulsion within the Cu 3*d* orbitals. In addition, we elucidate the crucial importance of the structural distortion of the CuO_2 chains in Li_2ZrCuO_4. This distortion is responsible for a reduction of both the interchain coupling and the NNN exchange J_2, as a consequence placing the system very close to the QCP.

II. METHODS

For the electronic-structure calculation a full-potential nonorthogonal local-orbital minimum-basis scheme

(FPLO5.00–19 and FPLO7.00–28),[22,23] within the local (spin) -density approximation [L(S)DA] was used. In the scalar relativistic calculations the exchange and correlation potential of Perdew and Wang was used.[24] We also applied the general gradient approximation (GGA) (Perdew-Burke-Ernzerhof[25]) for the exchange and correlation potential to check whether this influences the LDA results. Neither for the band structure nor for the total-energy differences we found any significant changes. For the basis the following states were taken into account: Cu($3s3p$)/$4s4p3d$, Li $1s$/($2s2p$)+$3d$, O($2s2p3d$), Zr($4s4p$)/($5s5p4d$) (notation: *semicore states/valence states*). The Cu $3s3p$, Li $1s$, and Zr $4s4p$ states were treated as semicore states due to the large extension of their wave functions. The unoccupied states Li $2p3d$, O $3d$, and Zr $5p$ were considered as hybridization states to complete the basis. All lower laying states were treated as core states. To ensure accuracy of the total energy 300 k points in the irreducible part of the Brillouin zone were used.

To model the Li(1) split position of the system (see below), we employed the virtual-crystal approximation (VCA) and coherent-potential approximation (CPA). Alternatively supercells with different Li(1) orders have been studied. To treat the strong on-site Coulomb repulsion for Cu $3d$ orbitals explicitly, the L(S)DA+U method[26] with U_{3d} in the representative range from 5.5 to 8.0 eV and $I=1$ eV for the intraatomic exchange have been used.

To study some aspects of the magnetic properties of the system a tight-binding (TB) model was derived from the LDA calculations to find the transfer integrals for a single-band effective extended Hubbard model which subsequently has been mapped onto a corresponding three-dimensional Heisenberg model. In addition, exact diagonalization studies of a five-band pd extended Hubbard model and its mapping onto the 1D-Heisenberg model using finite open Cu_nO_{2n+2} clusters have been carried out.

III. STRUCTURE

The γ phase of Li_2ZrCuO_4 (Refs. 21 and 27) crystallizes in an orthorhombic space group and is shown in Fig. 1(a). The compound contains distorted CuO_4 plaquettes which are arranged as edge-shared CuO_2 chains with an Cu-O-Cu bond angle of 94.13°. These edge-shared CuO_2 chains form layers together with the Li(2) atoms in the yz plane interconnected by ZrO_6 octrahedra. The alternating arrangement of the connecting ZrO_6 octrahedra lead to the deviation of the CuO_2 chains from the ideal planar geometry. In Fig. 1(b) the deflection of the O atoms from the chain plane is illustrated in detail.

As the CuO_4 plaquettes exhibit a localized, effective spin $\frac{1}{2}$, their linking and surrounding is of main importance for the formation of the magnetic ground state. A first structural analysis suggests sizable ferromagnetic NN exchanges caused by the close to 90° Cu-O-Cu bond angle according to the Goodenough-Kanamori-Anderson rule, provided the direct Cu-Cu transfer integral can be ignored.[28]

A further structural characteristic of the γ phase is a split position for Li(1) which is placed between the chain layers.

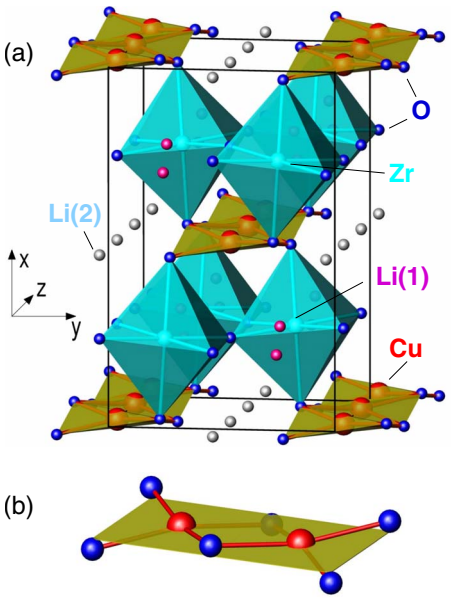

FIG. 1. (Color online) (a) Crystal structure of Li_2ZrCuO_4: chains of edge-shared CuO_4 plaquettes (yellow) run along the z direction and are connected by ZrO_6 octraheda (light blue). The fully occupied Li(2) site (gray) lies in the chain plane. The Li(1) split position (pink) alternates with the ZrO_6 octahedra. (b) Section of the Cu-O chain: the O atoms of a plaquette are deflected from the mirror plane (shown in yellow).

The distance of the Li(1) atoms from the high-symmetry position[29] is 0.37 Å. While the influence of the split position of Li(1) [corresponding to 50% disorder within a classical picture, ignoring possible tunneling processes of Li(1) between the two sites of the split position] to the magnetic properties is investigated carefully, we neglect the small disorder of 3–5 % at the Li(2) and Cu site in our theoretical calculations as a good approximation.

It is well known that in the vicinity of a QCP small changes in any parameter can be of crucial relevance for the ground state realized by the system. Therefore, the above-mentioned structural peculiarities of Li_2ZrCuO_6 raise the following two questions especially related to their influence on the electronic and magnetic properties. (i) How does the modeling of the Li(1) split position influences the calculated ground state? As there exists no standard procedure in band-structure codes to treat split positions we suggest various classical (i.e., within the adiabatic approximation) approaches. (ii) To which extend does the distortion of the CuO_4 plaquettes influence the placement of the compound in the J_1–J_2 phase diagram? Therefore a fictitious structure with ideal planar chain geometry was also considered.[30]

IV. RESULTS AND DISCUSSION

A. Modeling the Li(1) split position

The vicinity of Li_2ZrCuO_4 to a QCP requires a careful check of the structural description of the compound as a basis for our theoretical calculation. Therefore the treatment of the Li(1) split position might be crucial, although the dif-

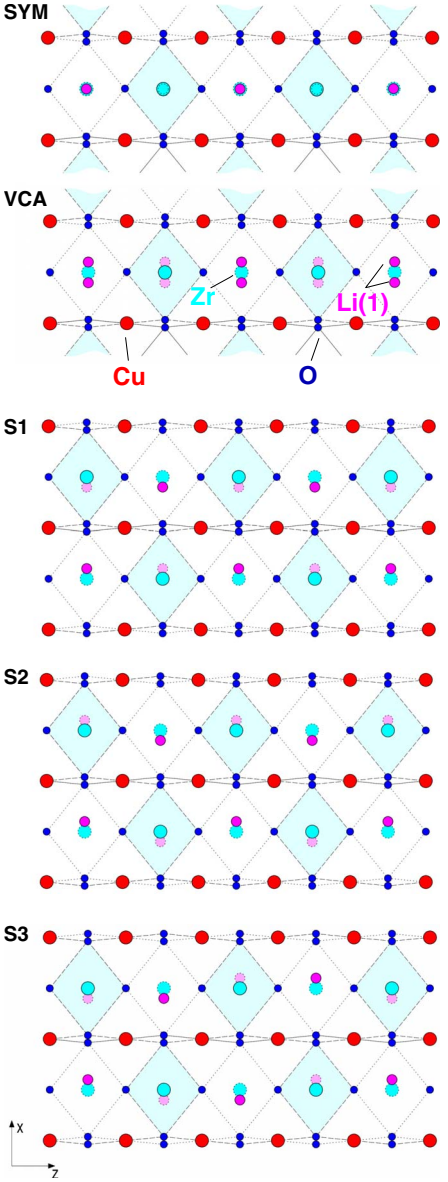

FIG. 2. (Color online) Different structural models to treat the Li(1) split position. From top to bottom: SYM—high-symmetry position for Li(1), VCA—both sites occupied by partial Li(1) atoms, S1 to S3—supercells with different Li(1) pattern. In S1 and S2 the Li(1) atoms along the chains are shifted parallel while in S3 the Li(1) atoms alter along the chain direction. S1 and S2 differ in the Li(1) interchain arrangement. The slight tilting of the ZrO_6 octrahedra (see Fig. 1) is not depicted for the sake of simplicity (full lines foreground, dashed lines background).

ferent models may only exhibit subtle differences. In the following we suggest different models to handle the split position and discuss the results with respect to the influence of these model assumptions on the relevant states and related dispersions. (i) To start from the most simplest approximation we performed electronic-structure calculation for Li(1) placed at the high-symmetry position [see Fig. 2 (SYM)]. (ii) As an alternative structural model we carried out VCA calculations [see Fig. 2 (VCA)]. This approach occupies both sites of the split position simultaneously by a half of a Li atom. Each of this modified Li atoms is constructed by carrying the half number of valence electrons and a modified core to conserve charge. For the VCA calculations the distance between the two sites of the split position has to be enlarged to suppress the overlap of the Li valence states and ensure the convergence of the calculation.[31] Also asymmetric charge distributions between the two sites of a split position (as, e.g., 0.8 and 0.2 Li) lead to nearly identical dispersion of the relevant states as long as the total charge of one Li atom per split position is conserved. However, deviations of the total charge of a split position cause sizable changes in the electronic structure.

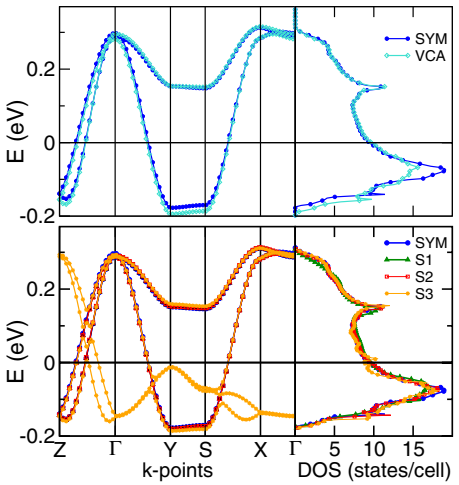

FIG. 3. (Color online) Calculated LDA density of states and band structure for the physical relevant states using different structural models for the Li split position. The comparison shows just minor differences.

This is also the reason why the description of the Li(1) split position by CPA fails, caused by the loss of charge balance at the split position in the later approximation. In contrast to the VCA, where the total charge at each split position sums up to one Li atom, the random occupation of the Li(1) split sites in the CPA also generates cases with empty and double occupied Li(1) sites with dramatic influence on the band structure and the total energy.

(iii) As both latter approaches do not touch the local symmetry, within a further model supercells with different Li(1) patterns have been calculated, breaking the local symmetry at the split position but suffer from long-range order (see Fig. 2 S1-S3). In the two upper panels the supercells were constructed by a reduction of the space-group symmetry. The Li(1) atoms along the chains are all shifted in the same direction while the Li(1) atoms of neighboring chains are parallel (S1) or antiparallel (S2) shifted. The third supercell (Fig. 2 S3) shows an alternating displacement of the Li(1) atoms along the chain obtained by a doubling of the cell in y direction.

The resulting bands and density of states for the different structural models show a very similar total behavior (see Fig. 3). Small deviations in VCA calculations can be observed in the bonding region of the valence band around −5.5 and −2.0 eV (not shown) in comparison to the high-symmetry model. These differences can be understood by the influence of the two modified Li cores to the crystal potential and the corresponding shift of Li-O states.

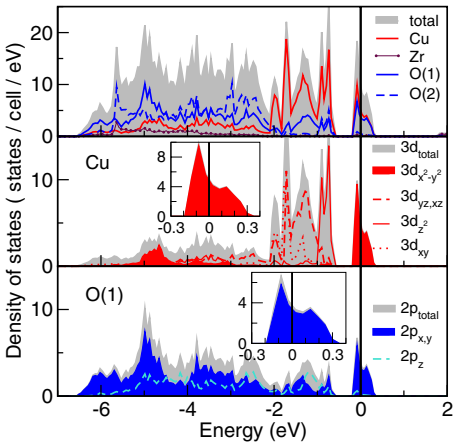

FIG. 4. (Color online) Calculated atom- and orbital-resolved density of states (LDA) for Li_2ZrCuO_4 applying the SYM model for the Li(1) split position (see text). The Li contribution to the valence band is negligible. Cu and O dominate the antibonding $dp\sigma^*$ band.

Comparing the density of states and LDA band structure for the antibonding $dp\sigma^*$ states, which are relevant for the magnetic exchanges and therefore the magnetism of the system, we found only tiny differences. (i) The VCA model results in a slightly larger bandwidth compared to the other models. (ii) The high-symmetry and supercell models nearly fit perfect. The additional bands of the S3 supercell with an alternating Li pattern can be understood due to the doubling of the primitive cell having its origin in the symmetry breaking of the Li pattern.

B. Electronic structure and magnetic properties

As the different structural models for the Li(1) split position show no significant difference in behavior for the relevant low-energy states (see Fig. 3), the electronic structure and the microscopic magnetic model are discussed for the SYM model as a good representative for all different structural models. To estimate more quantitatively the differences caused by the choice of the structural model the results for the SYM and the VCA models are compared.

In Fig. 4 the atom- and orbital-resolved density of states for Li_2ZrCuO_4 are shown. The valence band has a width of about 7eV, comparable with other chain cuprates and is dominated by Cu and O states, especially at the lower edge of the valence band around −6 eV (bonding states) and at the energy range close to zero (antibonding states). States of the Zr-O octrahedra appear in the middle part of the valence band. Their contribution to the states close to the Fermi energy is negligible.

The metallic character of the LDA results is in contradiction to the experimentally observed insulating ground state. This effect is a well known shortcoming of the LDA as it underestimates the strong correlations in the Cu 3*d* states. The related strong Coulomb repulsion on Cu sites can be considered explicitly by a model approach (e.g., a single-band Hubbard model using tight-binding parameters derived from the LDA) or by LDA+U calculations. Both methods were applied in this study and lead to an insulating ground state in agreement with the experimental data. Nevertheless, the LDA calculation delivers important insights into the electronic structure and provides the relevant bands for the development of a microscopically based picture for the magnetic ground state of Li_2ZrCuO_4.

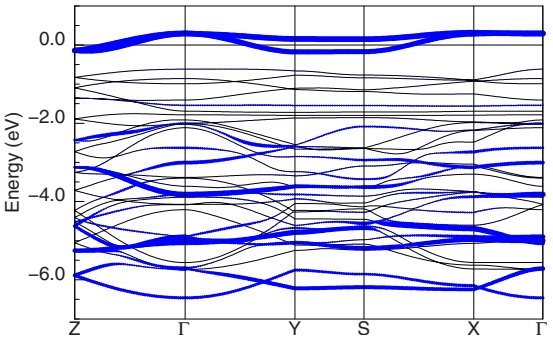

FIG. 5. (Color online) Valence band together with the band characters of the Cu 3*d* and O 2*p* antibonding states (blue) indicated by the linewidth. The band at Fermi energy is dominated by Cu and O antibonding $dp\sigma^*$ states.

The well-separated states around the Fermi energy are of main interest as they determine the magnetism of the system. These states are dominated by the in-plane orbitals of the CuO_4 plaquettes corresponding to the antibonding $dp\sigma^*$ states (see two lower panels in Fig. 4). The distortion of the plaquettes from an ideal planar chain geometry does not affect significantly the band characters of the antibonding $dp\sigma^*$ states. The hybridization with out-of-plane states is very small and does not differ from compounds with ideal planar CuO_2 chains.

In Fig. 5 the band structure of the valence band together with the Cu $3d_{x^2-y^2}$ and O $2p_{x,y}$ characters are shown. The antibonding $dp\sigma^*$ bands (see Fig. 6 left) show their main dispersion along the chain direction (Z-Γ) and in the chain

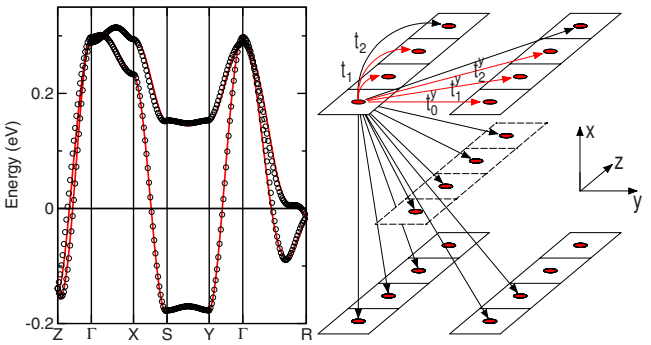

FIG. 6. (Color online) Left: comparison of the calculated band structure (black dots) and the least-square fit (red line) of the TB model. Right: considered hoppings for the TB model. The leading interactions are labeled and highlighted by red colors.

TABLE I. Resulting hopping integrals from TB fits for different structural models.

t_i/meV	t_1	t_2	t_0^y	t_1^y	t_2^y
SYM	−42	−56	−26	14	−25
VCA	−44	−55	−25	15	−26
FIC	−86	−92	−49	24	−21

plane (Γ-Y,S-X) indicating the leading magnetic exchanges in the layers. Perpendicular to these directions the dispersion is small, suggesting small exchanges between the chain layers.

To unravel the hierarchy of exchanges in the system as well as to estimate a cutoff for negligible long-range exchanges in further supercell calculations, an effective one-band model was fitted to the antibonding $dp\sigma^*$ bands. Effective hoppings for Cu-Cu distances up to 12 Å are considered (see Fig. 6 right) and calculated using a least-square-fit procedure. The resulting TB fit and the LDA bands are in perfect agreement (see Fig. 6 left).

All obtained transfer integrals larger than 5 meV are summarized in Table I. We found the main hoppings between NN and NNN along the chains and three considerable interchain hoppings in the chain plane. Comparing the SYM results with results from the VCA model, we see that the differences in the hopping integrals are very small and in the same order as the accuracy of the TB fit procedure. This indicates that the chosen structural model for the Li(1) split position is irrelevant for the calculated coupling constants of $Li_2Cu\,ZrO_4$. Taking into account the strong Coulomb repulsion in a model approach we construct from our TB model a single-band Hubbard model (with a typical value[32] $U_{\mathrm{eff}}=4.2$ eV for edge-shared CuO_2 chains) which can be mapped subsequently onto a Heisenberg model. We find $J_1^{\mathrm{AFM}}=1.7\pm0.1$ meV for the NN exchange and $J_2^{\mathrm{AFM}}=3.0\pm0.1$ meV for the NNN exchange.[33]

The exchange parameters resulted from the effective TB model disregard the FM contributions to the exchanges which are, however, expected between NN plaquettes in the compound due to the close to 90° bond angle Cu-O-Cu along the chains. Naturally, these FM interactions are included in LDA+U calculations. To evaluate J_1 and J_2 on a quantitative level, we performed a series of supercell calculations. The comparison of the total energies of these supercells with different spin arrangements[34] and a subsequent mapping onto a Heisenberg model leads to a FM NN exchange $J_1^{TOT}=-11.2$ meV and an AFM NNN exchange $J_2^{TOT}=2.2$ meV. The ground states of the compound is determined by the ratio $\alpha=-J_2^{TOT}/J_1^{TOT}=0.22\pm0.03$ that would result in a FM-ordered ground state in close vicinity of a QCP ($\alpha=0.25$). The variation of U_{3d} from 5.5 to 8.0 eV in the LDA+U calculation does not change this behavior qualitatively, although for the smaller U values a slightly increased α is obtained.[35] Besides a possible small error in the calculated exchange parameters, the experimentally observed spiral state from NMR data[36] might result due to the sizable interchain couplings $J_0^y=4(t_0^y)^2/U_{\mathrm{eff}}\sim0.6$ meV, $J_1^y\sim0.2$ meV and $J_2^y\sim0.6$ meV that both stabilize long-range order.

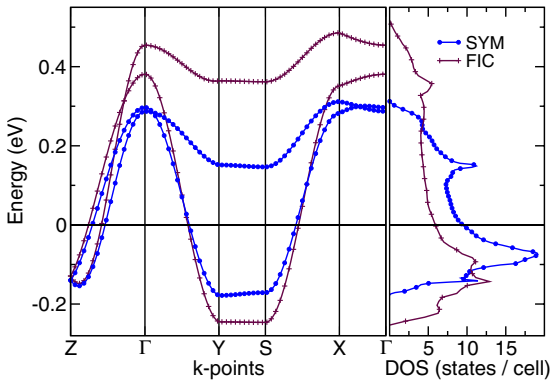

FIG. 7. (Color online) Comparison of band structure and density of states at Fermi energy for both chain geometries. The small displacement of O atoms from the mirror plane leads to a decrease in the band dispersion.

C. Influence of chain buckling

Whereas the different treatment of the Li(1) split position does not influence the band structure and the corresponding magnetic model essentially, the role of the distortion of the CuO_4 plaquettes [see Fig. 1(b)] remains to be addressed: how much does the nonplanar geometry of the chains influence the balance of the NN, NNN, and interchain couplings and the resulting placement of the compound in the J_1-J_2 phase diagram, especially its vicinity to the QCP? For a fictitious planar chain,[30] changes are expected since a changed Cu-O-Cu bond angle (changed by about 0.8°) will influence J_1^{TOT} and the different orientation of the antibonding $pd\sigma^*$ "molecular orbital" will alter J_2^{TOT}. Since these changes are hardly predictable quantitatively from structural considerations only, we apply our mapping approach also to a fictitious compound with ideal planar CuO_2 chains.

In Fig. 7 the resulting antibonding $dp\sigma^*$ bands and the related density of states for this fictitious structure are shown. For a planar chain geometry we obtain an about 50% larger bandwidth but a very similar shape of the bands compared with the real structure. On first glance, this suggests a scaling of the leading hopping parameters only. Our TB fit yields nearly a doubling of the hopping integrals as listed in Table I, thus a dramatic change of the corresponding exchange terms can be expected. To take into account the large FM contributions to J_1^{TOT}, we carried out LDA+U calculations for the same supercells used before.[34]

Surprisingly, we find a nearly unchanged NN exchange J_1^{TOT}, but only due to the compensation of the increased individual contributions J_1^{FM} and J_1^{AFM} (see Table II). Since the

TABLE II. Total and partial exchange integrals for different structural models from TB model and LDA+U calculation ($U_{3d}=7.5$ eV).

J_i/meV	J_1^{TOT}	J_2^{TOT}	J_1^{AFM}	J_1^{FM}	J_2^{AFM}	J_2^{FM}
SYM	−11.2	2.2	1.7	−12.9	3.0	−0.8
VCA	−10.6	2.5	1.8	−12.4	2.9	−0.4
FIC	−10.2	5.9	7.0	−17.2	8.0	−1.1

FM contribution J_2^{FM} to J_2^{TOT} remained small—as for the real structure—it basically scales like $J_2^{\mathrm{AFM}} \sim 4t_2/U_{\mathrm{eff}}$. Thus, we obtain a large change in J_2^{TOT} and consequently in the frustration ratio $\alpha \sim 0.6$ for the planar chains. In consequence, the ratio $\alpha = -J_2/J_1$ depends strongly on structural details of the local Cu-O environment. This is especially important regarding the vicinity of the system to the QCP. On the other hand this sensitivity of α to the chain buckling may provide the opportunity of manipulating the ground state of the system selectively by substitution or external pressure.

Unfortunately, a planar chain arrangement leads also to a sizable increase in the interchain coupling. This can be understood as the decrease in buckling increases the interchain overlap of the O orbitals belonging to the $pd\sigma^*$ states. This way, a tendency toward long-range order is stabilized, although the quantitative influence of interchain couplings to the ground state is sparsely considered in the literature.[37–39]

D. Stability of the Li(1) split position

Although the different treatments of the Li(1) split position yield no significant influence on the magnetic exchange parameters the split position may influence other properties of the compound. Related to the split position, the local symmetry or disorder could modulate the pitch angle of the helical state or be crucial for the formation of a possible multiferroic phase. Furthermore, ^{7}Li NMR and complex dielectric measurements reveal a glasslike ordering of the Li(1) ions below $T_g = 100$ K.[40] Thus, using our supercells simulating different types of Li(1) order (see Fig. 2), we tackled the questions whether a tendency to a static Li(1) order can be supported by calculations.

For the purpose of computational feasibility, we restricted ourselves to a fourfold cell (32 atoms).[41] The comparison of the total energy for the different ordered Li(1) patterns (SYM, S1, S2, S3) favors energetically the high-symmetry model (SYM) with a single Li(1) position. The second lowest in energy is the structure with alternating Li(1) displacement along the chain direction (S3). For this Li(1) arrangement, the dependence of the total energy on the displacement is depicted in Fig. 8. The resulting curve does not indicate a double-well potential as expected for a Li(1) split position but a minimum around the high-symmetry position and a harmonic behavior (see inset Fig. 8) up to almost 0.3 Å Li(1) displacement. According to our calculations, for the experimentally suggested Li(1) split position (marked by the arrow in Fig. 8) only slight anharmonic effects could be expected. We also investigated whether the strong Coulomb repulsion on the Cu site could be the reason for the discrepancy between the single Li(1) position suggested by the calculations and the experimental split position using LDA+U. With U_{3d} in the range from 5 to 7.5 eV we do not obtain any significant changes in the position of the minimum and the slope of the curve, suggesting that the correlations at the Cu site play only a minor role for a possible Li(1) order.

So far our calculations with a fixed lattice [apart from Li(1)] cannot support the split position but favor the high-symmetry solution (SYM). The discrepancy with the experiment that observed a glasslike Li(1) ordering below 100 K, may have the following origins: (i) dynamic effects that violate the adiabatic approximation used in the calculations or (ii) a correlated Li(1)-O(1) position without long-range order that would be difficult to detect in x-ray diffraction experiments. An investigation of these effects is beyond the scope of the present study but should be carried out in future since it might be crucial for the final picture of the compound.

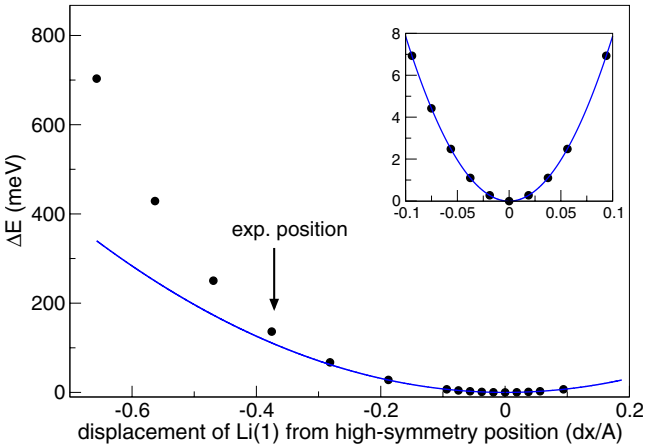

FIG. 8. (Color online) Energy difference depending on the displacement of the Li(1) atom from the high-symmetry position. The experimental observed displacement of 0.4 Å is indicated by an arrow. The inset shows a harmonic (second order) fit to the calculated energy differences for small displacements from the equilibrium position (±0.1 Å). The same fit is shown in the main panel, indicating deviations from the harmonic behavior at larger Li(1) elongations.

E. Cluster calculations

In order to provide an independent microscopic interpretation of the exchange integrals reported above, we performed exact diagonalization studies for the commonly used five-band extended *pd* Hubbard model for finite open Cu_nO_{2n+2} clusters. The most reliable way to choose a reasonable parameter set by fitting various spectroscopic experiments cannot be used here due to the lack of single crystals and available experimental data. Since no parameter set for the five-band *pd* model for a buckled chain geometry is available, we considered only the fictitious planar case (FIC) without any O buckling. This way, a direct comparison to the band-structure-derived results (FIC) should be more reliable. Thus, we started from an available parameter set known for the well-studied closely related sister compound Li_2CuO_2 with planar CuO_2 chains.[42,43] Then, only two Hamiltonian parameters—the mean Cu-O on-site difference $\Delta_{pd} = 3.5$ eV (3.75 eV) and $K_{pd} = 54$ meV (81 meV)—have to be slightly lowered to obtain consistency with the band-structure results for the exchange integrals J_1 and J_2 reported above. For comparison the Li_2CuO_2 parameters are given in brackets.[44] The slightly smaller Δ_{pd} is in line with the slight increase in the Cu-O distance by about 2% along the CuO_2 chains for Li_2ZrCuO_4 compared to Li_2CuO_2.

With these parameters the title compound exhibits a charge gap of about 2.35 eV as expected for an undoped

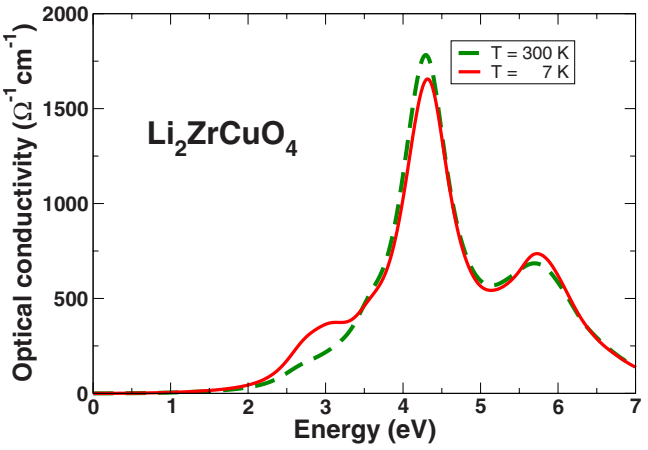

FIG. 9. (Color online) Optical conductivity of Li_2ZrCuO_4 within the five-band extended Hubbard model for a Cu_5O_{12} cluster.

cuprate. Therefore all eigenstates below that energy are spin states which can be described also reasonably well by a Heisenberg Hamiltonian. In case of a Cu_5O_{10} cluster we deal with ten spin states. Mapping for instance these ten spin states onto a 1D J_1-J_2-J_3-Heisenberg model,[45] we arrive then at $J_1=-10.6$ meV, $J_2=5.9$ meV, and $J_3=-0.3$ meV close to the values (FIC) given in Table II. Notice that our mapping on larger clusters with five Cu sites is considered to be more accurate than the determination of J_1 from a Cu_2O_4 dimer and J_2 from a Cu_2O_8 pseudotrimer, where the central Cu has been removed.[46]

In the context of the lower value of J_1 compared with Ref. 20 we would like to mention that from a microscopic point of view J_1 depends strongly on the adopted value of the direct ferromagnetic Cu-O exchange parameter K_{pd}. Within perturbation theory it occurs already in the second order whereas the antiferromagnetic superexchange due to deviations from the 90° and/or due to different crystal fields seen by the O orbitals along and perpendicular to the chain direction as well as the ferromagnetic Hund's-rule coupling and the O sites occur in the fourth order, only.[47] Analytically and numerically one obtains a linear dependence. Unfortunately, at present there is no consensus about a reliable value of K_{pd} based on microscopic considerations. Therefore it is frequently treated as fitting parameter to reproduce empirical or otherwise determined values of J_1 just as done here. For other CuO_2 edge-shared chain cuprates K_{pd} values in between 50 and 110 meV have been employed by various authors.[20,42,43,46,48] In our previous work on Li_2ZrCuO_4 (Ref. 20) 70 meV has been adopted, thus with the given above 54 meV we are near to the lower bound of so far used K_{pd} values. The former value was based on 1D fits of the magnetic susceptibility $\chi(T)$ and of the magnetic specific heat $c_v(T) \approx c_p(T)$, which might be significantly affected by the ignored interchain interaction. Due to the vicinity to the critical point the calculated 1D saturation field at $T=0$ K is very small on the order of 4–5 T. Hence, the experimentally measured saturation field of about 30 T (at low temperature) is clearly dominated by the interchain interaction in accord with our calculated sizable interchain couplings (see Sec. IV B).

In order to stimulate optical measurements and for a further experimental check of the applied Hamiltonian parameters we calculated (see Fig. 9) the in-chain optical conductivity for 300 and 7 K using the technique presented in Ref. 42. We draw attention to the strong temperature effect near 3 eV between low (7 K) and room temperature (300 K). This phenomenon is related to the different optical response in different initial spin states. For relatively small exchange integrals J_1 and J_2 the thermal population of these spin states changes markedly in the mentioned temperature range between zero and room temperature. Since the NN exchange J_1 (FIC) is mostly unchanged compared to the buckled structure (SYM, VCA), a strong temperature dependence of the optical conductivity should hold for the real compound.

Further investigations to settle the value of J_1 are highly desirable not only to get access to the Hamiltonian parameters[49] but also to check for renormalization and creation of longer-ranged couplings due to strong enough spin-phonon interaction.[50] The strong coupling of the exchange parameter J_2 to the O buckling, indicated by our band-structure calculations (see Table II), opens room for such a scenario.

V. CONCLUSIONS AND SUMMARY

To summarize, applying LDA and LDA+U band-structure calculations as well as exact diagonalization studies of an extended pd Hubbard model for large Cu_nO_{2n+2} clusters ($n=5$), that were finally all mapped onto a Heisenberg model, we obtain a consistent, microscopically based picture: (i) Li_2ZrCuO_4 can be understood as a quasi-1D chain compound with FM NN J_1 and AFM NNN J_2 exchange in close vicinity to a QCP. (ii) We find sizable interchain couplings that should be relevant for the magnetic ground state of the system, especially due to the vicinity of the system to a critical point where the impact of the leading exchange parameters on the ground state gets small. (iii) Calculations for a fictitious structure with planar chains indicate that the balance between J_1 and J_2 depends heavily on structural details, especially on the magnitude of the CuO_2 chain buckling. (iv) This also applies for the interchain coupling which is strongly increased for the fictitious planar geometry.

Our findings suggest that the buckling of the CuO_2 chain is crucial for the vicinity to the QCP, therefore it should be possible to tune the system toward that point by chemical substitution at the Zr site or by external pressure. On the other hand, it would be desirable to decrease the interchain coupling for which the orientation of the CuO $pd\sigma$ orbitals is more relevant than interatomic distances according to our results. Thus, a search for good quasi-1D systems should turn toward crystal structures where the chains are arranged in a strongly nonplanar pattern.

Our simulations indicate that the Li(1) split position has only a negligible direct influence on the spin system, assuming that all other atoms of the structure are fixed to their experimental position. In particular, our calculations do not support the experimental observation of a glassylike order for Li(1) on this split position[40] since it yields a single Li(1)

position as most energetically favorable. However, an indirect influence of the Li(1) position on the spin system is possible: taking into account a possible relaxation of the neighboring oxygen atom in the CuO_2 chain could result in a sizable modification of the exchange parameters as shown by the strong influence of this O position on the leading exchange terms. Another possible origin of the discrepancy concerning the Li(1) position could arise from dynamic and nonadiabatic effects that are beyond the scope of the present study.

ACKNOWLEDGMENTS

We acknowledge the DFG (Emmy-Noether program, H.R.) and the Grant No. DR269/3-1 (S.-L.D., J.M.), the German-Israel foundation (H.R.), and the ASCR Project No. AVOZ10100520 (J.M.) for financial support. The ZIH and the IFW Dresden are acknowledged for the use of their computer facilities. We thank O. Janson, D. Kasinathan, H. Eschrig, N. M. Plakida, A. S. Moskvin, and R. Kuzian for fruitful discussions.

[1] R. McKenzie, Science **278**, 820 (1997).
[2] G. Misguich and P. Sindzingre, Eur. Phys. J. B **59**, 305 (2007).
[3] D. Johnston, *Normal-State Magnetic Properties of Single-Layer Cuprate High-Temperature Superconductors and Related Materials* (North-Holland, Amsterdam, 1997), Vol. 10.
[4] R. Melzi, P. Carretta, A. Lascialfari, M. Mambrini, M. Troyer, P. Millet, and F. Mila, Phys. Rev. Lett. **85**, 1318 (2000).
[5] R. Melzi, S. Aldrovandi, F. Tedoldi, P. Carretta, P. Millet, and F. Mila, Phys. Rev. B **64**, 024409 (2001).
[6] H. Rosner, R. R. P. Singh, W. H. Zheng, J. Oitmaa, S.-L. Drechsler, and W. E. Pickett, Phys. Rev. Lett. **88**, 186405 (2002).
[7] H. Rosner, R. R. P. Singh, W. H. Zheng, J. Oitmaa, and W. E. Pickett, Phys. Rev. B **67**, 014416 (2003).
[8] A. Bombardi, J. Rodriguez-Carvajal, S. Di Matteo, F. de Bergevin, L. Paolasini, P. Carretta, P. Millet, and R. Caciuffo, Phys. Rev. Lett. **93**, 027202 (2004).
[9] R. Shpanchenko, V. Chernaya, A. A. Tsirlin, P. Chizhov, D. Sklovsky, E. Antipov, E. Khlybov, V. Pomjakushin, A. Balagurov, J. Medvedeva, E. E. Kaul, and C. Geibel, Chem. Mater. **16**, 3267 (2004).
[10] K. Oka, I. Yamada, M. Azuma, S. Takeshita, K. H. Satoh, A. Koda, R. Kadono, M. Takano, and Y. Shimakawa, Inorg. Chem. **47**, 7355 (2008).
[11] U. Nitzsche, S.-L. Drechsler, and H. Rosner (unpublished).
[12] Recent inelastic neutron-scattering data arXiv:0909.5687 yield $\alpha=0.31$ for Li_2CuO_2 and suggest that the ferromagnetic in-chain ordering in this compound is stabilized by the antiferromagnetic interchain interactions.
[13] A. A. Gippius, E. N. Morozova, A. S. Moskvin, A. V. Zalessky, A. A. Bush, M. Baenitz, H. Rosner, and S.-L. Drechsler, Phys. Rev. B **70**, 020406(R) (2004).
[14] S.-L. Drechsler, J. Málek, J. Richter, A. S. Moskvin, A. A. Gippius, and H. Rosner, Phys. Rev. Lett. **94**, 039705 (2005).
[15] M. Enderle, C. Mukherjee, B. Fak, R. Kremer, J. A. Broto, H. Rosner, S.-L. Drechsler, J. Richter, J. Malek, A. Prokofiev, W. Assmus, S. Pujol, J.-L. Raggazzoni, H. Rakoto, M. Rheinstädter, and H. M. Rønnow, Europhys. Lett. **70**, 237 (2005).
[16] T. Masuda, A. Zheludev, A. Bush, M. Markina, and A. Vasiliev, Phys. Rev. Lett. **92**, 177201 (2004).
[17] L. Capogna, M. Mayr, P. Horsch, M. Raichle, R. K. Kremer, M. Sofin, A. Maljuk, M. Jansen, and B. Keimer, Phys. Rev. B **71**, 140402(R) (2005).
[18] S.-L. Drechsler, J. Richter, A. Gippius, A. Vasiliev, A. Bush, A. Moskvin, Y. Prots, W. Schnelle, and H. Rosner, Europhys. Lett. **73**, 83 (2006).
[19] M. Hase, I. Terasaki, and K. Uchinokura, Phys. Rev. Lett. **70**, 3651 (1993).
[20] S.-L. Drechsler, O. Volkova, A. N. Vasiliev, N. Tristan, J. Richter, M. Schmitt, R. Rosner, J. Málek, R. Klinger, A. A. Zvyagin, and B. Büchner, Phys. Rev. Lett. **98**, 077202 (2007).
[21] C. Dussarrat, G. C. Mather, V. Caignaert, B. Domengès, J. G. Fletcher, and A. R. West, J. Solid State Chem. **166**, 311 (2002).
[22] The total-energy calculations for the Li(1) position (Sec. IV D) have been carried out with both versions to ensure the independence from the basis set.
[23] K. Koepernik and H. Eschrig, Phys. Rev. B **59**, 1743 (1999).
[24] J. P. Perdew and Y. Wang, Phys. Rev. B **45**, 13244 (1992).
[25] J. P. Perdew, K. Burke, and M. Ernzerhof, Phys. Rev. Lett. **77**, 3865 (1996).
[26] H. Eschrig, K. Koepernik, and I. Chaplygin, J. Solid State Chem. **176**, 482 (2003).
[27] Since in Ref. 21 and in the ICSD(59618) the lattice parameters and internal coordinates are inconsistent or erroneous, we explicitly provide the parameters used in the calculations: space group *Cccm* (66), $a=9.385$ Å, $b=5.895$ Å, $c=5.863$ Å, Cu(0.0, 0.0, 0.5), Li(1)(0.21, 0.75, 0.0), Li(2)(0.0, 0.5, 0.25), Zr(0.25, 0.25, 0.0), O(1)(−0.0246, 0.228, 0.5), O(2)(0.2662, 0.0, 0.25).
[28] J. Kanamori, Prog. Theor. Phys. **17**, 177 (1957).
[29] For the high-symmetry position (SYM) Li(1) is placed at (0.25, 0.75, 0.0).
[30] O(1) was placed at (0.0, 0.228, 0.5). This structural variation decreases the Cu-O bond length by 0.01 Å, and increases the Cu-O-Cu bond angle along the edge-shared chain by 0.8°.
[31] The experimentally determined distance between the two possible sites of a split position is 0.757 Å. For the VCA calculation the distance has been enlarged to 1.314 Å.
[32] F. Parmigiani, L. Sangaletti, A. Goldoni, U. del Pennino, C. Kim, Z.-X. Shen, A. Revcolevschi, and G. Dhalenne, Phys. Rev. B **55**, 1459 (1997).
[33] The error bars take into account the differences between the two Li(1) models (see Fig. 2, top) and the numerical errors of the fitting procedure.
[34] We doubled the unit cell along the chain direction and stabilized the following periodic spin arrangements to calculate J_1 and J_2: $\uparrow\uparrow\uparrow\uparrow, \uparrow\downarrow\uparrow\downarrow, \downarrow\uparrow\uparrow\uparrow$.
[35] For $U_d=5.5$ eV and $U_d=8.0$ eV we obtain $J_1=-16.7$ meV, $J_2=4.1$ meV, $\alpha=0.25$ and $J_1=-10.1$ meV, $J_2=1.9$ meV, $\alpha=0.19$, respectively.
[36] Y. Tarui, Y. Kobayashi, and M. Sato, J. Phys. Soc. Jpn. **77**,

043703 (2008).
[37] R. Zinke, S.-L. Drechsler, and J. Richter, Phys. Rev. B **79**, 094425 (2009).
[38] H. Katsura, S. Onoda, J. H. Han, and N. Nagaosa, Phys. Rev. Lett. **101**, 187207 (2008).
[39] S. Furukawa, M. Sato, Y. Saiga, and S. Onoda, J. Phys. Soc. Jpn. **77**, 123712 (2008).
[40] E. Vavilova, A. Moskvin, Y. Arango, A. Sotnikov, V. Kataev, S.-L. Drechsler, O. Volkova, A. Vasiliev, and B. Büchner, EPL **88**, 27001 (2009).
[41] Besides the very small energy differences compared to the large total energy for different Li(1) elongations from the equilibrium position, the main problem for larger cells is the rather bad convergency behavior. The bad convergency is related to the well-known problem of "charge shuffling" between (with respect to their charge density) almost identical but crystallographically formally different atoms.
[42] J. Málek, S.-L. Drechsler, U. Nitzsche, H. Rosner, and H. Eschrig, Phys. Rev. B **78**, 060508(R) (2008).
[43] J. Málek, R. Kuzian, S. Nishimoto, M. Knupfer, and S.-L. Drechsler (unpublished).
[44] The remaining parameters of the five-band extended Hubbard model read U_d=8.5 eV, U_p=4.1 eV, U_{pp}=2.9 eV, K_p=0.6 eV (Hund's rule coupling on O-sites), V_{pd}=0.65 eV (intersite Coulomb interaction, neglected in Ref. 42), ε_d=0, ε_{p_x}=3.6 eV (in chain) and ε_{p_y}=3.4 eV (perpendicular to the chain). The transfer integrals read $t_{p_y d}$=0.662 eV, $t_{p_x d}$=0.765 eV, $t_{p_x p_x}$=0.84 eV, $t_{p_y p_y}=-t_{p_x p_x}/4$ in chain direction as well as 0.96 and −0.24 eV in transversal direction (see also Ref. 46, notice the different notation of the chain axis (see Fig. 6).
[45] The accuracy of the least-square fit for the differences between the Hubbard and Heisenberg eigenenergies amounts 10^{-6}.
[46] Y. Mizuno, T. Tohyama, S. Maekawa, T. Osafune, N. Motoyama, H. Eisaki, and S. Uchida, Phys. Rev. B **57**, 5326 (1998).
[47] H. Eskes and J. H. Jefferson, Phys. Rev. B **48**, 9788 (1993).
[48] M. Braden, G. Wilkendorf, J. Lorenzana, M. Ain, G. J. McIntyre, M. Behruzi, G. Heger, G. Dhalenne, and A. Revcolevschi, Phys. Rev. B **54**, 1105 (1996).
[49] Similar problems occur also for J_2 except the fact that it is hardly affected by K_{pd} but by the much smaller value K_{pp}. In the present calculation we have therefore ignored K_{pp} as it is usually done in the literature.
[50] A. Weisse, G. Wellein, and H. Fehske, Phys. Rev. B **60**, 6566 (1999).